Characterizing functional relationships between anthropogenic and biological sounds: a western New York state soundscape case study

Jeffrey W. Doser · Kristina M. Hannam · Andrew O. Finley

Abstract

Context Roads are a widespread feature of landscapes worldwide, and road traffic sound potentially makes nearby habitat unsuitable for acoustically communicating organisms. It is important to understand the influence of roads at the soundscape level to mitigate negative impacts of road sound on individual species as well as subsequent effects on the surrounding landscape.

Objectives We seek to characterize the relationship between anthropogenic and biological sounds in western New York and assess the extent to which available traffic data explains variability in anthropogenic noise.

Methods Recordings were obtained in the spring of 2016 at 18 sites throughout western New York. We used the Welch Power Spectral Density (PSD) at low frequencies (0.5–2 kHz) to represent anthropogenic noise and PSD values at higher frequencies (2–11 kHz) to represent biological sound. Relationships were modeled using a novel two-stage hierarchical Bayesian model utilizing beta regression and basis splines.

Results Model results and map predictions illustrate that anthropogenic noise and biological sound have an inverse relationship, and anthropogenic noise is greatest in close proximity to high traffic volume roads. The predictions have large uncertainty, resulting from the temporal coarseness of public road data used as a proxy for traffic sound.

Conclusions Results suggest that finer temporal resolution traffic sound data, such as crowd-sourced time-indexed traffic data from geographic positioning systems, might better account for observed temporal changes in the soundscape. The use of such data, in combination with the proposed modeling framework, could have important implications for the development of sound management policies.

J. W. Doser (✉) · A. O. Finley
Department of Forestry, Michigan State University, East Lansing, MI, USA
e-mail: doserjef@msu.edu

K. M. Hannam
Department of Biology, State University of New York (SUNY) Geneseo, Geneseo, NY, USA

A. O. Finley
Department of Geography, Environment, and Spatial Sciences, Michigan State University, East Lansing, MI, USA

Introduction

Roads are a widespread feature of most landscapes worldwide, with road networks growing dramatically in the past 100 years. In the United States alone, there

are over 6.3 million kilometers of public roads, most of those (80%) found in rural areas (Forman et al. 2003). Nowhere in the United States is very far from a road, with the farthest straight line distance from a road in the lower 48 states being a spot in Wyoming 21 miles from the nearest road (Project Remote 2019). Since 1970, the traffic on US roads has at least tripled to almost 5 trillion vehicle kilometers traveled per year (Barber et al. 2010). Habitat fragmentation caused by roads is detrimental to wildlife due to direct mortality via wildlife-vehicle collisions, exposure to pollutants, and exposure to sound from road traffic (Parris and Schneider 2008; Barber et al. 2011; McClure et al. 2013; Snow et al. 2018). Thus, while roads alter habitats and landscapes structurally, impacts of roads on animal diversity and abundance can also be impacted by altered acoustic environments (Katti and Warren 2004; McClure et al. 2013).

Acoustic space, or the soundscape, is an essential resource for both terrestrial and marine animals (Pijanowski et al. 2011a; Farina 2018). Animals utilize the auditory spectrum for a variety of functions, including reproduction (McGregor 2005), predation and to warn of danger (Marler and Slabbekoorn 2003; Templeton 2006; Ridley et al. 2007; Sloan and Hare 2008), and to find food (Knudsen and Konishi 1979; Rice 1982; Neuweiler 1989). The sounds organisms produce are collectively called biological sound, which combine together with abiotic sounds from the earth, like wind and rushing water, and human-produced sounds (anthropogenic noise) to form the soundscape (Pijanowski et al. 2011a). Road sound may be the most pervasive form of anthropogenic noise impacting natural habitats and contributes sound with particular characteristics to the soundscapes of those habitats. Sound from a road is a linear rather than a point source (Katti and Warren 2004), the sound from traffic tends to be low frequency (typically below 2 kHz) and high amplitude, and the timing of road sound in some places can vary greatly over time (e.g., rush hour peaks) and depend on traffic load (Slabbekoorn and Ripmeester 2008).

Traffic sound and other sources of anthropogenic noise have created soundscapes with novel acoustic characteristics in which acoustically communicating animals send and receive signals. High amounts of anthropogenic noise reduce the perception of biologically important sound (Barber et al. 2010) and are thought to have negative effects on both cognitive

processes (Potvin 2017) as well as behavior (Brumm and Slabbekoorn 2005). Traffic sound often masks auditory signals, limiting or preventing senders and receivers from communicating effectively, a phenomenon that is well-documented (Brumm and Slabbekoorn 2005; Patricelli and Blickley 2006), particularly for birds and frogs. Traffic sound was shown to cause physiological stress and impair breeding behavior in multiple frog populations throughout the world (Tennessen et al. 2014), and similar effects have been demonstrated in birds (Warren et al. 2006; Ortega 2012). Some bird species are able to respond to anthropogenic noise by adapting characteristics of their song to overcome masking. A study on Song Sparrows (*Melospiza melodia*), found a positive correlation between the minimum frequency of a male's song and the amplitude of low-frequency background noise in a range of urban environments (Wood and Yezerinac 2006), suggesting the organisms are attempting to adapt to increased low frequency sound by changing the pitch of their songs to overcome masking. However, responses to anthropogenic noise are species specific, and not all species are able to change signal frequency or amplitude in a short term response to increased sound in the environment (Brackenbury 1978; Oberweger and Goller 2001; Patricelli and Blickley 2006). Further, even organisms that are able to adapt their signals may suffer from reduced fitness (Phillips and Derryberry 2018), suggesting anthropogenic noise can have negative effects even on the species that change their signals in response to increasing sound (Patricelli and Blickley 2006). An alternative response to anthropogenic noise is for species to avoid habitats where it impacts the soundscapes, a conclusion drawn from tests of the "phantom road" effect (McClure et al. 2013) and observations of changes in species abundances near roads (Fahrig and Rytwinski 2009).

Without proper management of anthropogenic noise, the negative impacts could cause changes in species composition with potentially far reaching effects on the ecosystem. Thus, it is necessary to analyze the relationship between biological sound and anthropogenic noise and understand how it changes across temporal and spatial gradients in order to accurately predict how anthropogenic noise will influence the species comprising the biological sound. More specifically, the identification of anthropogenic noise "hot spots" in space and time will allow natural

resource managers and others to pinpoint the times and locations in which human sound should be mitigated to maintain the integrity of local ecosystems (Ortega 2012). A potential first step in addressing these complex problems is developing a model that quantifies the relationship between biological sound and prominent sources of anthropogenic noise, such as road sound.

Ecoacoustics researchers (Sueur et al. 2008; Farina and Gage 2017) have developed a number of acoustic indices, such as the Acoustic Complexity Index (ACI) (Pieretti et al. 2011), Acoustic Diversity Index (ADI) (Villanueva-Rivera et al. 2011), Bioacoustic Index (BI) (Boelman et al. 2007), and Normalized Difference Soundscape Index (NDSI) (Kasten et al. 2012) to quantify soundscapes and understand how biological sound relates to anthropogenic noise. NDSI was developed to compare the relative amounts of anthropogenic noise and biological sound within an environment (Kasten et al. 2012) and has been shown to correlate well with landscape characteristics despite its relative simplicity (Fuller et al. 2015), and is thus a reasonable measure to further characterize the relationship between anthropogenic noise and biological sound across different spatio-temporal gradients. The NDSI is built using the Welch power spectral density (PSD) (Welch 1967) for 1 kHz frequency bins within the recording.

The NDSI and PSD are useful tools for tracking spatio-temporal changes in soundscapes (Pijanowski et al. 2011a; Mullet et al. 2016). However, soundscape data present some unique challenges that potentially cannot be addressed using these indices and simple statistical models. For example, the data used in this study are multivariate (partitioned into frequencies associated with anthropogenic and natural sounds), compositional (frequency ranges sum to total sound at a given location and time), non-Gaussian, and are highly correlated across time. Soundscape data are also typically sparsely sampled in space, highly correlated across space, and often comprise high-dimensional continuous time series for short time intervals with large intervening time gaps. While contemporary statistical literature offers modeling theory for such data complexities (Clark 2007; Hobbs and Hooten 2015), applied methodology and software are not yet available in the field of ecoacoustics. Application of statistical models that can address these complexities can lead to improved inference and

prediction on important soundscape variables across space and time, quantified by statistically valid estimates of uncertainty.

In this study, we propose a hierarchical Bayesian modeling approach to assess the spatial distribution of biological sound and anthropogenic noise in western New York soundscapes in relation to roads and traffic density. Hierarchical Bayesian models (HBMs) offer an intuitive framework to decompose complex ecological problems into logical parts (data, process, and parameters) (Berliner 1996; Cressie et al. 2009). The framework is ideal for drawing inference about soundscapes as it can accommodate high-dimensional, multivariate, compositional data with time and space dependence. Specifically, our objectives are to: (1) characterize the functional relationship between anthropogenic noise and biological sound; (2) assess the extent to which available traffic data explains variability in anthropogenic noise; (3) develop a methodology to deliver statistically valid maps of anthropogenic noise and biological sound that reflect the relationship identified in Objective 1 with accompanying uncertainty quantification.

Materials and methods

Study location and data collection

Recording sites were located in nine forest patches in western New York. The forest plots included two arboretums managed by colleges (State University of New York at Geneseo and Monroe Community College), two forest plots owned and managed by the Genesee Valley Conservancy, two forest plots in the town of Brighton, and one forest plot each in the towns of Avon, Conesus, and Rush. Forest plot locations were chosen along an urban–rural gradient to provide soundscapes with varying exposure to levels of anthropogenic noise.

We obtained recordings at two locations within each of the nine forest plots, resulting in 18 total recording sites. The two locations within each site were chosen to provide recordings of soundscapes at varying distances to the nearest major road. From May to June 2016 we obtained three 30 min recordings at each recording site in the morning (between 6 and 8 am), afternoon (between 12 and 2 pm), and evening (between 6 and 9 pm), resulting in a total of 54 30 min

recordings. All recordings were taken on weekdays and specific recording times within the specified sampling periods were chosen randomly. We recorded in stereo at a sampling rate of 44.1 kHz using a Song Meter SM4 from Wildlife Acoustics (Wildlife Acoustics 2012) mounted on a tripod 1 m above the ground using the built-in omnidirectional microphones with a sensitivity of -36 ± 4dB. We discarded the last minute of each 30 min recording as a result of extraneous sound. Each 29 min recording was broken up into 29 consecutive 1-min sound bites, resulting in a total of $n = 18$ sites $\times$ 3 times per day $\times$ 29 sound bites $= 1566$ observations. We recorded on days with similar weather conditions during which birds are known to communicate (i.e., no rain, minimal wind) to minimize any influence of weather on the observed soundscape patterns.

We used basic scatter plots and standard regression functions in R (Bates et al. 2015) to assess the influence of the day of the recording and the time of a morning recording from sunrise on the relationship between biological sound and anthropogenic noise. We did not find large amounts of variability in this relationship across the differing factor levels, and so we do not include them as covariates in the subsequent modeling framework.

Soundscape metrics

Recordings were manually analyzed using a sampling scheme for rapid soundscape analysis (Bobryk et al. 2016) to determine the most common acoustically communicating organisms in the soundscapes. The analysis revealed the soundscapes contained varying amounts of anthropogenic noise depending on the site and were dominated by avian species, the most common species including American Robin (*Turdus migratorius*), Cedar Waxwing (*Bombycilla cedrorum*), Yellow Warbler (*Setophaga petechia*), Red-eyed vireo (*Vireo olivaceus*), and Eastern Wood-Pewee (*Contopus virens*).

Each 1 min soundscape recording was summarized using the PSD as computed by Welch (Welch 1967). The PSD represents the amount of soundscape power within each frequency band in units of watts/kHz (Fig. 1). Each PSD value was vector normalized to account for differences in recorder setting (i.e., system sensitivity, frequency response) and to facilitate

comparison of PSD values obtained at different sites (Joo et al. 2011). Here we chose to use the Welch spectrum to compute the PSD in units of watts/kHz as opposed to computing the PSD in units of dB re $20\,\mu$Pa^{2}Hz^{-1} (Merchant et al. 2015) as this method has been employed in numerous terrestrial soundscape studies to create indices of the amount of biological sounds, anthropogenic noise, and a ratio between the two types of sound (Joo et al. 2011; Kasten et al. 2012; Fuller et al. 2015; Farina and Gage 2017; Buxton et al. 2018a, b; Rajan et al. 2019). We computed the PSD for each 1.5 kHz frequency band between 0.5 and 11 kHz (i.e., a total of seven 1.5 kHz bands), where each value ranged from 0 (no sound) to 1 (filled with sound).

Anthropogenic noise commonly occurs in the frequency ranges between 0.5 and 2 kHz (Napoletano 2004; Joo et al. 2011; Kasten et al. 2012). Thus, we used the normalized PSD from the 0.5 to 2 kHz band to represent the amount of anthropogenic noise in each recording following the technique of Kasten et al. (2012) and the sum of the 1.5 kHz width PSD values from 2 to 11 kHz to represent the amount of biological sound in each recording. We assume all sound below the frequency of 2 kHz is anthropogenic noise. Such an assumption is generally not safe in western New York because several species communicate in these frequency ranges (e.g., Red Fox (*Vulpes vulpes*), Northern Flicker (*Colaptes auratus*), American Crow (*Corvus brachyrhynchos*), Common Raven (*Corvus corax*)). However, the manual analysis found only one common species (American Crow) communicating in this frequency range in our data set, suggesting that using the PSD from the 0.5 to 2 kHz band will be a fairly reasonable approximation for the total amount of anthropogenic noise in the soundscapes recorded in this study. The anthropogenic and biological sound values were scaled to the range of 0–1 watts/kHz by dividing by the total number of frequency bins involved in their computation (1 and 6, respectively). We used the soundecology (Villanueva-Rivera and Pijanowski 2018), tuneR (Ligges et al. 2018), and seewave (Sueur et al. 2008) packages within the R Statistical Software (R Core Team 2019) environment to compute these measures. PSD values were averaged over the left and right channels to obtain a single value of anthropogenic noise and biological sound for each recording.
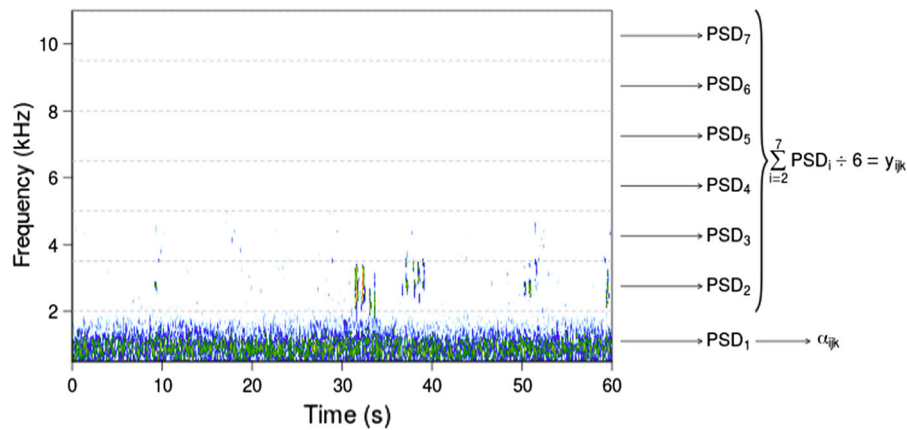
Fig. 1 Computation of biological sound (y_{ijk}) and anthropogenic noise (α_{ijk}) values using the power spectral density for a single recording minute (*i*) at a single location (*j*) at a single time of day (*k*)

To further assess our frequency range assumptions for biological and anthropogenic sounds, a subset of recordings was analyzed to determine the proportion of biological sound in the 0.5–2 kHz band. Two one minute recordings for each combination of site and time period were analyzed (108 one minute recordings). The analysis revealed biological sounds were scarcely present in the 0.5–2 kHz band, with a median of 0.9 s of each minute containing audible biological sounds (First Quartile: 0 s, Third Quartile: 3.48 s), and a total of 50 recordings containing no audible biological sounds in the 0.5–2 kHz band (Fig. 2). The

biological sounds within the 0.5–2 kHz range also tended to be of low amplitude compared to the anthropogenic noise in the same recording, and thus their impact on the PSD would be minimal. Anthropogenic noise was sometimes present above the 2 kHz region, especially in the 2–3 kHz region. Exploratory data analysis revealed this was in the soundscapes primarily dominated with anthropogenic noise where the anthropogenic noise PSD value was > 0.95. Thus, we acknowledge the values for biological sound at high levels of anthropogenic noise may be overestimated. However, this would not change our results to a
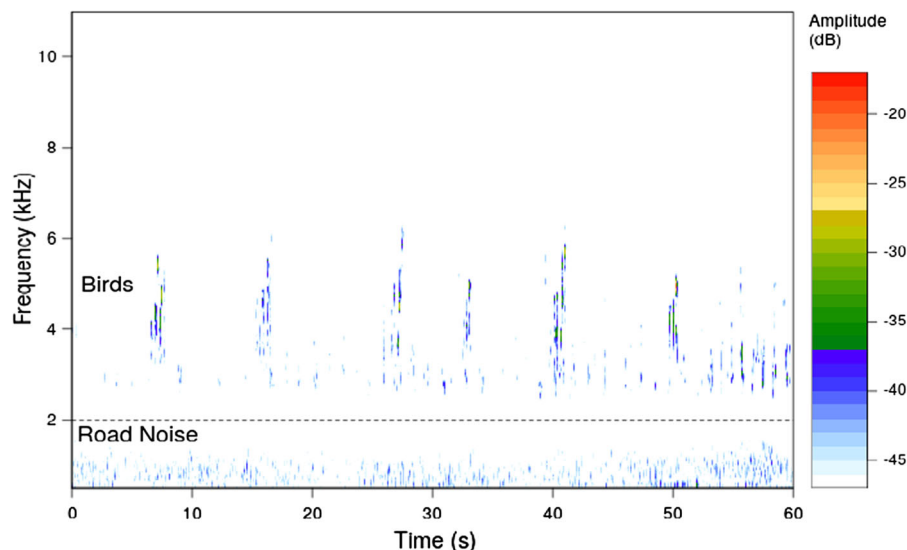

Fig. 2 Spectrogram of an example sound recording. The horizontal line represents the cutoff value used to separate anthropogenic and biological sounds

high degree, as the biological values at high levels of anthropogenic noise are already quite low (see data points in Fig. 5), and so we believe this assumption is valid for these specific soundscapes.

Road influence

To assess the influence of roads and traffic sound on the soundscapes we used public data from the New York State GIS Clearinghouse (NYS ITS GIS Program Office 2019) containing road locations and average speeds. A second data set was acquired from the New York State Department of Transportation (NYS Department of Transportation 2018) containing the average annual daily traffic (AADT) and an estimate of the percent of trucks on Federal and State highways, and on county and town roads. The roads from these data sets are plotted in Fig. 3, clearly showing the ubiquitousness of roads throughout western New York. We created a road covariate to quantify the road influence on the soundscape at any given location. This road covariate (RC) took into account 5 factors: (1) average speed; (2) distance of recording site to road; (3) AADT; (4) Percent of trucks; (5) shape of the road. To quantify the shape of the road, we broke each road into 10×10 m pixels, obtained the corresponding AADT, speed, and percent of truck values with each road pixel, and computed the distance of each road pixel within 600 m of a given recording site. The 600m boundary is an estimate of how far anthropogenic noise will travel through a forested landscape (Forman and Deblinger 2000; MacLaren et al. 2018).

We predicted average speed, AADT, and percent of trucks to have a positive relationship with anthropogenic noise and distance to have a negative relationship with anthropogenic noise. Thus, the road covariate is computed as follows for a given 10×10m pixel i:

$$RC_i = AADT + speed + truck - distance$$

The variables are scaled to provide approximately equal weight to all variables. The complete road covariate for a given recording site is then computed by summing the RC_i for all locations i within 600 m of the given recording site, thus accounting for the shape of the roads near a given recording site. This road covariate is visualized in the study region in Fig. 3, indicating the covariate is only high near roads, and highest near intersections in the Rochester area.

Quantification of roads was limited to the roads assessed by the New York State Department of Transportation. These data come primarily from 12,000 annual short traffic counts of 2–7 days of duration. More counts took place in urban areas than in rural and agricultural areas (NYS Department of Transportation 2018), which could potentially lead to the road covariate being an underestimate in rural and agricultural regions.
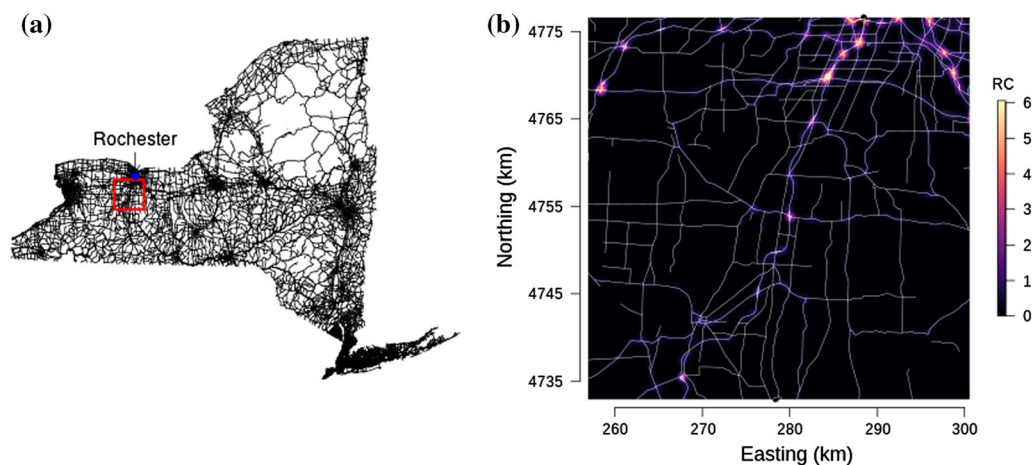

Fig. 3 Distribution of roads in New York State. **a** Public road data is displayed across all of NYS. **b** The road covariate is computed at a 30×30 m resolution for the boxed area

Model

We seek a model that: (1) provides parameter estimates and associated uncertainty regarding the relationship between biological sound and anthropogenic noise; (2) assesses the amount of anthropogenic noise variance explained by the road covariate; (3) enables biological sound and anthropogenic noise prediction with associated uncertainty. Importantly, we take the view that biological sound is conditional on anthropogenic noise, and both variables are observed with error. We considered three hierarchical Bayesian models of increasing complexity, henceforth referred to as Model 1, Model 2, and Model 3. Each model consisted of two stages. Stage 1 models anthropogenic noise as a function of the road covariate. Stage 2 models biological sound conditional on Stage 1 such that uncertainty in observed anthropogenic noise is appropriately propagated through the two stages for inferences and subsequent prediction (Lunn et al. 2013).

Consider the PSD value for anthropogenic noise $\alpha_{i,j,k}$ and the road covariate x_j, where $i = 1, 2, \ldots, 29$ is the minute of the continuous 29-min recording, $j = 1, 2, \ldots, 18$ indexes recording site, and $k = 1, 2, 3$ indexes time of day. All first stage models use beta regression to account for the bounded support of $\alpha_{i,j,k}$ on [0, 1] and follow the mean and precision parameterization detailed in Ferrari and Cribari-Neto (2004).

Exploratory data analysis revealed the relationship between anthropogenic noise and the road covariate was non-linear and residuals (i.e., after accounting for the road covariate) were serially correlated with non-constant variance. These features were accommodated using cubic b-splines to obtain a smooth curve over the anthropogenic noise and road covariate functional relationship, and a temporally structured random effect to acknowledge the correlation among the 1-min anthropogenic noise sound bites over each 29 min recording. More specifically, the random effect followed a multivariate normal distribution with mean 0 and an AR(1) covariance matrix.

Inferences proceeded by assigning model parameters non-informative prior distributions then a Markov Chain Monte Carlo (MCMC) algorithm sampled from posterior distributions. The full hierarchical model for Model 1, including prior specifications, is detailed below ($[a \mid b]$ is the probability distribution of a conditional on b) :

Stage 1:

$$[\boldsymbol{\beta}_\alpha, \sigma_\alpha^2, \rho_\alpha, \phi_\alpha, w_{i,j,k} \mid x_j, \alpha_{i,j,k}] \propto$$

$$\prod_{i=1}^{29} \prod_{j=1}^{18} \prod_{k=1}^{3} \text{beta}(\alpha_{i,j,k} \mid g(\boldsymbol{\beta}_\alpha, x_j, w_{i,j,k})\phi_\alpha,$$

$$(1 - g(\boldsymbol{\beta}_\alpha, x_j, w_{i,j,k}))\phi_\alpha) \times$$

$$\text{multivariate normal}(w_{i,j,k} \mid 0, \sigma_\alpha^2 \boldsymbol{\Sigma}(\rho_\alpha)) \times$$

$$\text{inverse gamma}(\phi_\alpha \mid 2, 20000) \times$$

$$\text{inverse gamma}(\sigma_\alpha^2 \mid 2, 5) \times$$

$$\prod_{l=1}^{5} \text{normal}(\beta_{\alpha,l} \mid 0, 10000) \times$$

$$\text{uniform}(\rho_\alpha \mid 0.1, 1)$$

where $g(\boldsymbol{\beta}_\alpha, x_j, w_{i,j,k}) = \text{inverse logit}(\mathbf{Z}_{x_j}\boldsymbol{\beta}_\alpha + w_{i,j,k})$, $\mathbf{Z}_{x_j}$ is the row in the b-spline design matrix for the specific value of the road covariate x_j, $w_{i,j,k}$ is the random effect with mean 0 and an AR(1) covariance structure with variance σ_α^2, correlation ρ_α, and $n \times n$ matrix $\boldsymbol{\Sigma}$ (with block diagonal structure where each block is the covariance among 29 consecutive sound bites), $\boldsymbol{\beta}_\alpha$ are spline regression coefficients, and ϕ_α is the precision.

Point and interval estimates for parameters and fitted values were obtained from the joint posterior distribution (Gelman et al. 2004). Recall, the central role of the Stage 1 model is to explore the relationship between the road covariate and α, and propagate the uncertainty in α to the Stage 2 model for the biological sound. This was accomplished by obtaining M post burn-in samples of the fitted values from Stage 1, i.e., M $n \times 1$ vectors of $\hat{\boldsymbol{\alpha}}^{(m)} = (\hat{\alpha}_1^{(m)}, \hat{\alpha}_2^{(m)}, \hat{\alpha}_3^{(m)}, \ldots, \hat{\alpha}_n^{(m)})^\top$ where $m = 1, \ldots, M$, and by using them as the covariate in a similar mixed effect beta regression model for the biological sound, $y_{i,j,k}$. The overall structure of Stage 2 is exactly the same as Stage 1, with the exception that each MCMC iteration m fits the biological sound to a different sample $\hat{\boldsymbol{\alpha}}^{(m)}$. Stage 2 takes the following form, where all parameters are analogous to Stage 1:

Stage 2:

$$[\boldsymbol{\beta}_y, \sigma_y^2, \rho_y, \phi_y, v_{i,j,k} \mid \hat{\alpha}_{i,j,k}^{(m)}, y_{i,j,k}] \propto$$

$$\prod_{i=1}^{29} \prod_{j=1}^{18} \prod_{k=1}^{3} \text{beta}(y_{i,j,k} \mid g(\boldsymbol{\beta}_y, \hat{\alpha}_{i,j,k}^{(m)}, v_{i,j,k})\phi_y,$$

$$(1 - g(\boldsymbol{\beta}_y, \hat{\alpha}_{i,j,k}^{(m)}, v_{i,j,k}))\phi) \times$$

multivariate normal$(v_{i,j,k} \mid 0, \sigma_y^2 \Sigma(\rho_y)) \times$

inverse gamma$(\phi_y \mid 2, 2000) \times$

inverse gamma$(\sigma_y^2 \mid 2, 2) \times$

$$\prod_{l=1}^{8} \text{normal}(\beta_{y,l} \mid 0, 10000) \times$$

uniform$(\rho_y \mid 0.1, 1)$.

While Model 1 does accommodate the serial correlation among the 1-min sound bites, it does not acknowledge within day (i.e., morning, afternoon, and evening) repeated measures aspect of the sampling design. This within day covariance is explicitly taken into account in Model 2 by replacing the scalar variance parameters, σ_α^2 and σ_y^2, with a 3×3 covariance matrix, $\boldsymbol{\lambda}_\alpha$ and $\boldsymbol{\lambda}_y$, whose diagonal elements represent the random effect variance for the respective time period (morning, afternoon, evening) and whose off-diagonal elements represent the covariance between recordings in different time periods. Unlike in Model 1, this structure allows us to make inferences about similarities or differences between the soundscape recordings across the three time periods. The $\boldsymbol{\lambda}$'s are modeled with a non-informative inverse-Wishart prior with degrees of freedom 3 and a diagonal scale matrix with all diagonal elements equal to 0.1. We use Kronecker products to obtain the desired structure of the covariance matrix, and apply this structure in both Stages 1 and 2.

After examining output from Models 1 and 2, diagnostic plots showed observed versus fitted values exhibited heteroskedasticity and associate credible intervals were not appropriately capturing the variability. This non-constant variance was directly addressed in Model 3. For Stage 1, the heteroskedasticity resulted from the relationship between anthropogenic noise and the road covariate. This was remedied by fitting two separate precision parameters $\phi_{\alpha,l}$ and $\phi_{\alpha,u}$ the expression of which was controlled by an indicator function such that $\phi_{\alpha,l}$ is the

precision at values of the road covariate less than 2, while $\phi_{\alpha,u}$ is the precision at values of the road covariate greater than 2. While we could have formally estimated the indicator function break point parameter, it was clear from diagnostic plots that a road covariate value of 2 was adequate, see, e.g., Fig. 4. Both $\phi_{\alpha,l}$ and $\phi_{\alpha,u}$ are modeled with non-informative inverse gamma priors. In Stage 2, we model the precision parameter ϕ_y as a function of anthropogenic noise, specifically taking the form $\phi_{y,1} + \phi_2 \exp(\hat{\alpha}_{i,j,k})$. We modeled $\phi_{y,1}$ and $\phi_{y,2}$ using vague uniform priors from 0 to 10,000.

Prediction

We seek to develop statistically valid maps of anthropogenic noise and biological sound that reflect the relationships obtained from the three models with associated uncertainty quantification. We computed the road covariate as described previously across a square region in western New York (Fig. 3). The posterior predictive distribution for anthropogenic noise is

$$[\boldsymbol{\alpha}^* \mid \boldsymbol{\alpha}, \boldsymbol{x}] = \int_{-\infty}^{\infty} [\boldsymbol{\alpha}^* \mid \boldsymbol{\theta}_\alpha][\boldsymbol{\theta}_\alpha \mid \boldsymbol{\alpha}] d\boldsymbol{\theta}_\alpha \qquad (1)$$

where $\boldsymbol{\alpha}^*$ is a vector of anthropogenic noise values at new locations, $\boldsymbol{x}$ is a vector of road covariate values at new locations, and $\boldsymbol{\theta}_\alpha$ is a vector of Stage 1 parameters. Similarly, the posterior predictive distribution for biological sound is

$$[\boldsymbol{y}^* \mid \boldsymbol{y}, \hat{\boldsymbol{A}}] = \int_{-\infty}^{\infty} [\boldsymbol{y}^* \mid \boldsymbol{\theta}_y][\boldsymbol{\theta}_y \mid \boldsymbol{y}] d\boldsymbol{\theta}_y \qquad (2)$$

where $\boldsymbol{y}$ is a vector of biological sound values at new locations, $\hat{\boldsymbol{A}}$ is an $n^* \times M$ matrix, where n^* is the number of new locations to predict, and M is the number of post-burn MCMC iterations of the fitted values of Stage 1, and $\boldsymbol{\theta}_y$ is a vector of Stage 2 parameters.

The integrals in (1) and (2) are approximated using MCMC based composition sampling (see, e.g., Banerjee et al. 2014). Posterior predictive samples from $\boldsymbol{\alpha}^*$ and $\boldsymbol{y}^*$ were used to compute anthropogenic noise and biological sound medians and associated credible intervals.
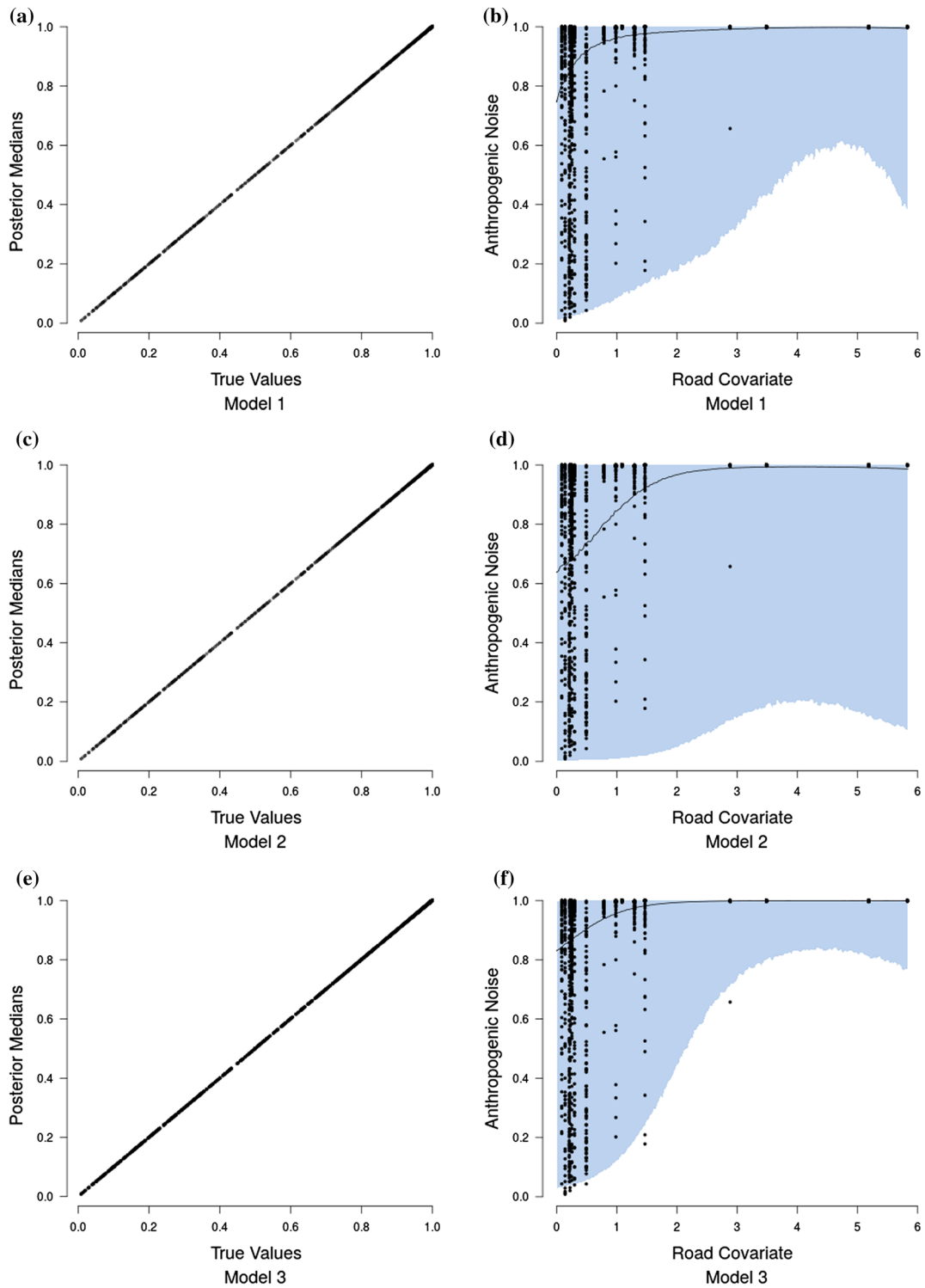
Fig. 4 Stage 1 model fits. 95% credible intervals are displayed as gray lines in (**a**), (**c**), and (**e**). Posterior medians of model fitted values are displayed in black and 95% credible intervals are displayed as the blue shaded regions in (**b**), (**d**), and (**f**)

Convergence diagnostics and model validation

Diagnostics were performed to ensure convergence of the MCMC chains. We used a combination of visual assessment of trace plots and an alternative version of the Gelman-Rubin diagnostic that does not assume normality of the correction factor (Brooks and Gelman 1998).

True assessment of the predictive ability of a model requires some form of hold out data that are not used for fitting the model. To accomplish this, we performed a k-fold cross validation technique with $k = 6$ (Vehtari and Lampinen 2002). This technique requires fitting the model k times, where each time the model is fit on n/k data points, where n is the length of the data set. Each run of the model fits on a different portion of the data, and predicts the remaining $n - n/k$ hold out values. Since these data are not used in the model fitting process, they represent true draws from the posterior predictive distribution that can be compared with the actual values of the data to assess the predictive capabilities of the model. We used the Continuous Rank Probability Score (Gneiting and Raftery 2007) and the Expected Log Pointwise Predictive Density (Vehtari et al. 2017) to compare the predictive capabilities of the model. Further, we computed the 95% coverage interval for each of the models, which gives us the percentage of the actual data values that fall within the 95% credible interval of the model.

Software implementation

MCMC samplers were written in C++ using an Adaptive-Metropolis-within-Gibbs algorithm (Roberts and Rosenthal 2009). Computationally expensive matrix operations were coded using the Intel Math Kernel Library (MKL) BLAS and LAPACK routines. Prediction and model validation were performed in both C++ and R utilizing the scoringRules package to compute the CRPS (Jordan et al. 2018). All subsequent analysis was performed in R (R Core Team 2019). Data and code are available on GitHub (https://github.com/doserjef/DHF20).

Results

Figure 4 shows the relationship between the road covariate and anthropogenic noise depends upon the value of the road covariate. When the road covariate is high, there are large amounts of anthropogenic noise, aligning with intuition and previous research suggesting that anthropogenic noise is higher in more urban areas (Pijanowski et al. 2011a, b). However, at low values of the road covariate we obtain essentially no information about anthropogenic noise in the soundscape. Candidate model parameter estimates are given in Table 1. Convergence diagnostics suggested rapid convergence for all model parameters with the exception of a few spline coefficients, β's, in Stage 1. Such lack of convergence is common in spline-based regression components, especially in the presence of an additive structured random effect (Wood and Yezerinac 2006; Hanks et al. 2015). This lack of convergence is of no concern because we are not interested in interpreting the individual spline basis function coefficients—we simply look to Stage 1 to adequately capture the uncertainty in observed anthropogenic noise, and characterize the relationship between anthropogenic noise and the road covariate.

Model fits are shown in Fig. 5 along with the estimated relationship between biological sound and anthropogenic noise. Generally, as anthropogenic noise increases, biological sound decreases, aligning with previous research (Pijanowski et al. 2011b). Model 3 performed best according to all model validation criteria; however, all models performed very well. Candidate model parameter estimates are given in Table 2. All Stage 2 model parameters showed strong convergence.

To ease interpretation, covariance matrix estimates are often best expressed as correlations. Converting each MCMC sample from the λ's posterior to a correlation provides access to the corresponding correlation matrix posterior, which is summarized in Tables 3 and 4 for Stages 1 and 2, respectively.

Because inference is primarily focused on estimating biological sound given anthropogenic noise in the soundscapes, we perform model comparison only for Stage 2 models. A sixfold-cross validation was used to compare candidate models' out-of-sample prediction using the CRPS and ELPD. High values of the ELPD and low values of the CRPS suggest a better model fit. We also report the percentage of points covered by the

Table 1 Stage 1 posterior parameter medians and 95% credible intervals, 50% (2.5%, 97.5%)

Parameter	Model 1	Model 2	Model 3
$\beta_{\alpha,0}$	1.12 (1.10, 1.15)	0.64 (0.60, 0.65)	1.59 (1.57, 1.61)
$\beta_{\alpha,1}$	3.71 (3.68, 3.74)	1.01 (0.93, 1.06)	2.46 (2.36, 2.54)
$\beta_{\alpha,2}$	3.84 (3.59, 4.05)	5.38 (5.00, 5.86)	7.40 (7.00, 7.59)
$\beta_{\alpha,3}$	6.83 (6.60, 7.41)	4.81 (4.45, 5.18)	6.81 (6.06, 7.45)
$\beta_{\alpha,4}$	4.37 (4.19, 5.28)	4.12 (3.90, 4.46)	6.44 (6.23, 6.63)
ϕ_{α}	232,161 (80,716, 878,895)	348,648 (105,344, 738,622)	–
$\phi_{\alpha,l}$	–	–	92,623 (37,579, 228,416)
$\phi_{\alpha,u}$	–	–	239,221 (68,653, 1976,045)
$\lambda_{\alpha,(1,1)}$	–	2.85 (2.58, 3.21)	2.23 (2.10, 2.54)
$\lambda_{\alpha,(2,1)}$	–	0.07 (-0.22, 0.36)	0.02 (-0.21, 0.25)
$\lambda_{\alpha,(3,1)}$	–	0.62 (0.29, 0.95)	0.46 (0.21, 0.73)
$\lambda_{\alpha,(2,2)}$	–	3.28 (2.96, 3.73)	2.63 (2.39, 2.92)
$\lambda_{\alpha,(3,2)}$	–	0.11 (-0.22, 0.44)	0.06 (-0.19, 0.32)
$\lambda_{\alpha,(3,3)}$	–	3.78 (3.39, 4.29)	3.01 (2.73, 3.36)
σ_{α}^{2}	8.38 (7.04, 10.23)	–	–
ρ_{α}	0.89 (0.87, 0.91)	0.92 (0.90, 0.94)	0.87 (0.85, 0.90)

Subscript in parentheses on λ_{α} indicate the row and column element in $\boldsymbol{\lambda}_{\alpha}$

95% credible intervals of the predicted biological sound versus anthropogenic noise relationship, which should ideally cover 95% of the data points (Table 5).

The models yield anthropogenic noise and biological sound prediction at the 29 min observation resolution for three times of the day. Such fine temporal resolution is likely not that useful from an assessment or management perspective. Hence, we summed each 29 min biological sound and anthropogenic noise posterior predictive sample, resulting in a posterior predictive distribution for the total anthropogenic noise and biological sound at each pixel across the study area for morning, afternoon, and evening. The median and range between the upper and lower 95% credible interval bounds for each pixel-level predictive distribution were mapped. Very little differences were detected among the models and between predictions at the morning, afternoon, and evening, and thus we only present posterior predictive maps for the afternoon soundscapes for Model 3 in Fig. 6.

Discussion

There is recent widespread recognition that anthropogenic traffic noise alters the acoustic habitat for many animal species (Barber et al. 2010, 2011; Buxton et al. 2017), and influences biodiversity within reach of that sound (Katti and Warren 2004; McClure et al. 2013). Acoustic soundscape recordings are now commonly used in the field of ecoacoustics to monitor natural soundscapes impacted by anthropogenic noise (Pijanowski et al. 2011b; Farina 2018). An important and complex challenge in ecoacoustics is to determine the impacts of road noise on biodiversity. As a potential first step to address this problem, we proposed a novel hierarchical Bayesian model to explore the relationships between public road data, anthropogenic noise, and biological sounds. Specifically, we developed three two-stage mixed effects beta regression models to assess the degree to which public traffic data explains variability in anthropogenic noise and to characterize the relationship between biological sound and anthropogenic noise in western New York soundscapes. The models were compared using inference delivered and out-of-sampled prediction. Models were then applied to provide anthropogenic noise and
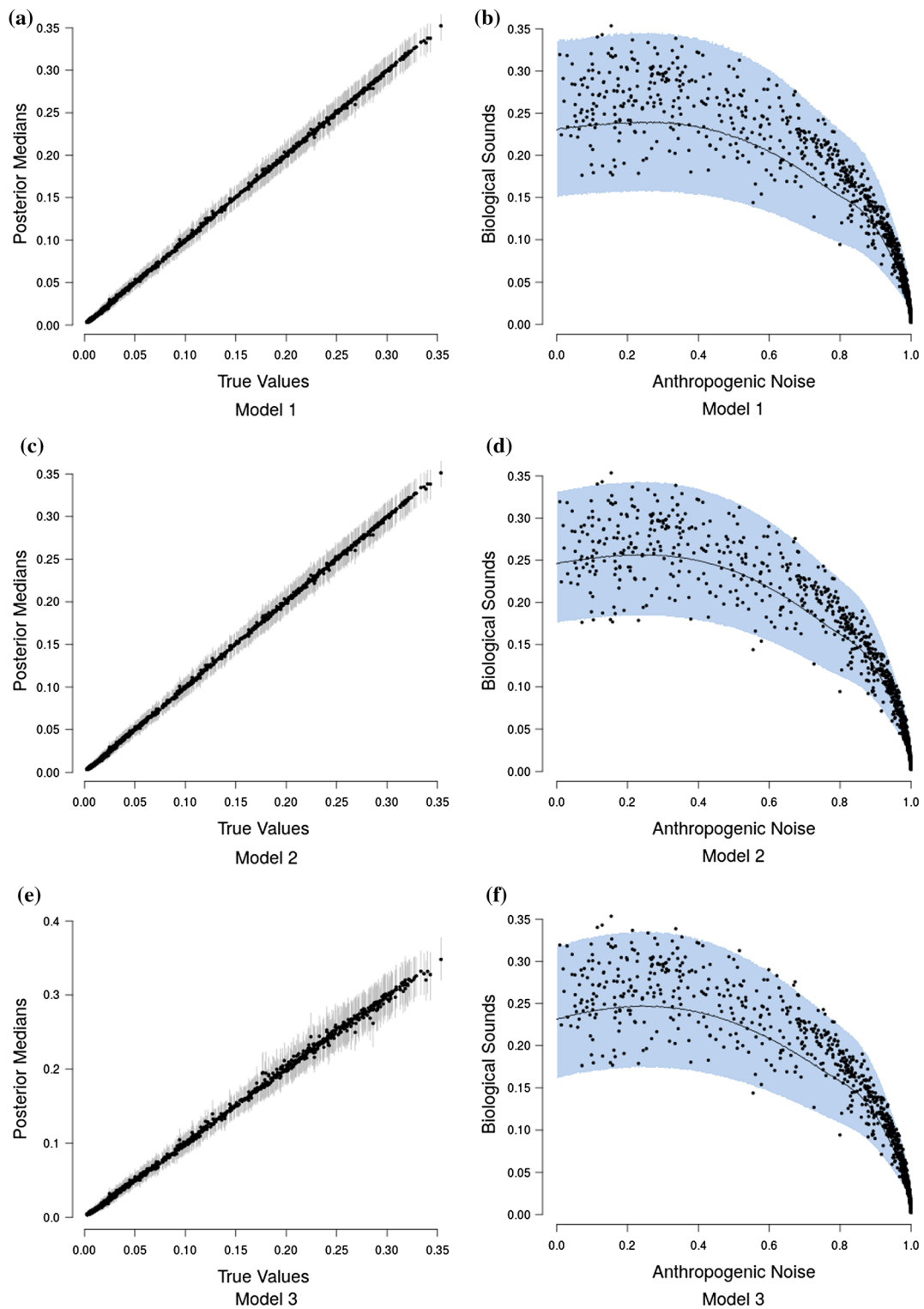
Fig. 5 Stage 2 model fits. 95% credible intervals are displayed as gray lines in (**a**), (**c**), and (**e**). Posterior medians of model fitted values are displayed in black and 95% credible intervals are displayed as the blue shaded regions in (**b**), (**d**), and (**f**)

biological sound predictive maps over a sample region in western New York using public road data. The predictive maps have large uncertainty in locations far from roads, resulting from the temporal coarseness of public road data used as a proxy for traffic noise. This suggests a need for finer temporal resolution traffic noise data. The use of such data, in combination with the proposed modeling framework, could have important implications for the development of soundscape and sound management policies.

Road noise is one of the most ubiquitous sources of anthropogenic noise (Barber et al. 2010; Project Remote 2019). In Stage 1 of our proposed modeling framework, we model the relationship between public road traffic data and anthropogenic noise to determine how well the public traffic data explains variability in anthropogenic noise (Fig. 4). Model results ultimately displayed the inability of the road covariate to explain variability in anthropogenic noise at low values. The large uncertainty in the relationship between anthropogenic noise and the road covariate is also evident in the predictions of anthropogenic noise given new values of the road covariate, as the credible interval widths are extremely large at areas where the road

covariate is low (Fig. 6). The large variation in the anthropogenic noise values at low levels of the road covariate could potentially be improved by incorporating important variables regarding the road surface type that likely influence the propagation of road sound throughout the environment, which were not available in the data sets used in this study. However, the data showed high variability in the anthropogenic noise values within each site, suggesting it is more likely that high variability in this relationship is a result of individual effects that are not accounted for by site level variables. These individual effects are

Table 3 Model 3 Stage 1 random effect correlation matrix posterior medians and 95% credible intervals, 50% (2.5%, 97.5%)

	Morning	Afternoon	Evening
Morning	–	–	–
Afternoon	0.01 (−0.08, 0.10)	–	–
Evening	**0.18 (0.08, 0.28)**	0.02 (−0.07, 0.11)	–

Boldface indicates parameter values not containing 0 in the associated 95% credible interval

Table 2 Stage 2 posterior parameter medians and 95% credible intervals, 50% (2.5%, 97.5%)

Parameter	Model 1	Model 2	Model 3
$\beta_{y,0}$	−1.16 (−1.26, −1.09)	−1.14 (−1.20, −1.11)	−1.21 (−1.26, −1.06)
$\beta_{y,1}$	−1.08 (−1.16, −0.96)	−1.01 (−1.06, −0.96)	−1.07 (−1.18, −0.98)
$\beta_{y,2}$	−1.01 (−1.08, −0.95)	−0.99 (−1.06, −0.91)	−1.07 (−1.12, −0.98)
$\beta_{y,3}$	−1.75 (−1.78, −1.71)	−1.71 (−1.76, −1.65)	−1.74 (−1.78, −1.70)
$\beta_{y,4}$	−1.87 (−1.91, −1.80)	−1.84 (−1.88, −1.78)	−1.91 (−1.95, −1.85)
$\beta_{y,5}$	−2.99 (−3.03, −2.96)	−2.98 (−3.02, −2.91)	−3.00 (−3.04, −2.96)
$\beta_{y,6}$	−3.49 (−3.54, −3.43)	−3.48 (−3.52, −3.43)	−3.54 (−3.59, −3.48)
$\beta_{y,7}$	−5.04 (−5.09, −4.99)	−5.06 (−5.11, −4.98)	−5.03 (−5.10, −5.00)
ϕ_y	7487 (5658, 9606)	6919 (5526, 9085)	–
$\phi_{y,1}$	–	–	128.68 (4.53, 542.99)
$\phi_{y,2}$	–	–	1343.38 (1072.11, 1596.93)
$\lambda_{y,(1,1)}$	–	0.21 (0.19, 0.23)	0.21 (0.19, 0.24)
$\lambda_{y,(2,1)}$	–	−0.004 (−0.03, 0.02)	−0.01 (−0.04, 0.02)
$\lambda_{y,(3,1)}$	–	0.05 (0.03, 0.08)	0.06 (0.03, 0.09)
$\lambda_{y,(2,2)}$	–	0.20 (0.18, 0.22)	0.20 (0.18, 0.23)
$\lambda_{y,(3,2)}$	–	0.007 (−0.02, 0.03)	0.02 (−0.02, 0.05)
$\lambda_{y,(3,3)}$	–	0.21 (0.19, 0.24)	0.21 (0.19, 0.24)
σ_y^2	0.06 (0.05, 0.07)	–	–
ρ_y	0.82 (0.78, 0.86)	0.74 (0.70, 0.79)	0.82 (0.76, 0.86)

Subscript in parentheses on λ_y indicate the row and column element in λ_y

Table 4 Model 3 Stage 2 random effect correlation matrix posterior medians and 95% credible intervals, 50% (2.5%, 97.5%). Boldface indicates parameter values not containing 0 in the associated 95% credible interval

	Morning	Afternoon	Evening
Morning	–	–	–
Afternoon	−0.06 (−0.20, 0.09)	–	–
Evening	**0.27 (0.14, 0.45)**	0.08 (−0.12, 0.22)	–

Table 5 Comparison of ELPD, CRPS, and 95% Coverage Intervals

	Model 1	Model 2	Model 3
ELPD	730.5	728.17	733.17
CRPS	0.0098	0.0097	0.0097
95% Coverage	95.66	92.85	94.96

likely a result of large variations in the number/type of automobiles on the road at any given minute of time. We listened to all recordings, and confirmed road sound was the most prominent source of anthropogenic noise, further suggesting the high variation of the relationship between the road covariate and the human sound is a result of high temporal variation in the number of cars on a given road, a phenomenon that is well-described in literature on traffic sound modeling (Conesel et al. 2005; Can et al. 2008). The use of models that incorporate the dynamic temporal changes of road sound across time could help account for the temporal changes in traffic and subsequent traffic sound if traffic data are limited as in this study (Can et al. 2008). Utilizing crowd-sourced traffic data from traffic and navigation apps (i.e., Google Maps, Waze) is an intriguing alternative that would enable more time-specific measures of traffic and subsequently the sound it produces. Such space-time data, in combination with the modeling frameworks proposed here, could result in near real-time maps of anthropogenic noise that could have important implications for the development of sound management policies.

Using spatially or temporally structured random effects in soundscape models can improve model accuracy when the data are limited and the researcher suspects there are individual effects causing variation not explained by the data (Clark 2007). In this study, the use of random effects allowed us to incorporate temporal dependence between recordings, obtain

accurate model fits, and predict anthropogenic noise and biological sound despite using a predictor (the road covariate) that does not explain large amounts of variation of anthropogenic noise.

Understanding the relationship between biological sounds and anthropogenic noise is an important initial step in determining the impact of anthropogenic noise on biodiversity. In Stage 2 of our modeling framework, we quantify the complex, non-linear relationship between biological sound and anthropogenic noise (Fig. 5). We modeled this relationship using three candidate models, each increasing in complexity. Table 5 shows that Model 3 has the highest ELPD, the lowest CRPS values, and the most accurate 95% coverage. This suggests that accounting for the repeated measures across time of day in the soundscape recordings as well as the non-constant variance in the data provides an improvement in the model.

Soundscapes are highly correlated across both space and time (Pijanowski et al. 2011b; Mullet et al. 2016) and thus a modeling framework that quantifies such correlations are important inferential tools. The additional time of day correlation estimates in Models 2 and 3 provide inference on the relationship between the soundscapes over the morning, afternoon, and evening recordings. For Model 3, Stage 1 (Table 3), we see the correlation between the random effects of the afternoon recordings with both the random effects of the morning and evening recordings are not different from 0 (i.e., 0 is contained within the 95% credible interval), whereas the correlation between morning and evening random effects are small but different from 0, with a posterior median of 0.18. This suggests that variations in anthropogenic noise not explained by the road covariate are similar in the morning and evening recordings, although the correlation coefficient of 0.18 suggests this is not a strong relationship. For Model 3, Stage 2 (Table 4), we see similar results in that the correlation between morning
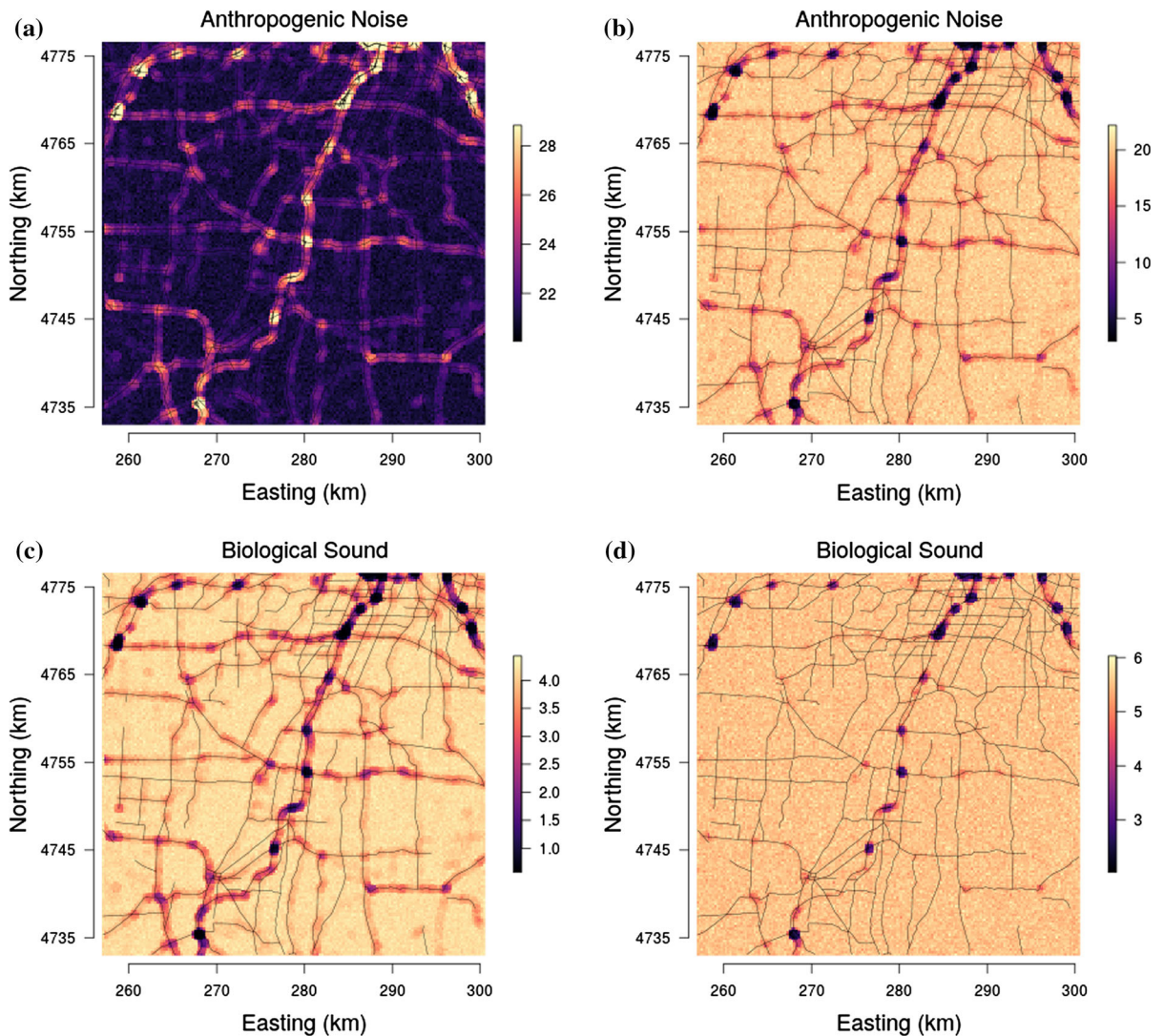
Fig. 6 Model 3 afternoon predictions of anthropogenic noise and biological sound over a sample region in western New York. Posterior medians are shown in (**a**) and (**c**), while posterior 95% credible interval widths are shown in (**b**) and (**d**)

and evening recordings is different from 0, with a posterior median of 0.27, suggesting that variations in biological sound not explained by anthropogenic noise are more similar in the morning and the evening recordings than they are between the afternoon recordings and either the morning or evening recordings. This is likely a result of the dawn and dusk choruses, which are captured by the morning and evening recording time periods, respectively. Thus, we see that Model 3 provides slight improvements in terms of the model validation criteria, in addition to providing insights into the temporal relationships

between biological sound and anthropogenic noise that are not available from the more simple Model 1.

To illustrate how our modeling framework can be used to predict anthropogenic and biological sounds over larger spatial areas, we provide soundscape maps of a sample region in western New York at a 250 × 250 m resolution where we predict anthropogenic noise and biological sound from public road data. Visualization of the posterior median suggests that biological sound is highest in areas farther away from roads, while anthropogenic noise is high in regions of more concentrated and highly used roads. This aligns

with previous research and intuition, as the probability of detection of avian species vocalizations is lower closer to roads (Parris and Schneider 2008) and anthropogenic noise increases with the degree of urbanization (Pijanowski et al. 2011a). However, a visualization of the 95% credible interval widths shows that there are large amounts of uncertainty associated with these estimates at areas with low anthropogenic noise, largely a result of the inability of anthropogenic noise to be accurately predicted at low levels of the road covariate. Thus, inference drawn from these maps is limited due to our lack of certainty.

Despite the fact that there is a clear negative relationship between biological sound and anthropogenic noise, we see that past a given distance from the road the predictions of biological sound are all very similar. In this study, we were solely interested in the relationship between anthropogenic noise and biological sound and the ability of public road data alone to serve as a predictor. If more accurate predictions of biological sound are desired, it will be important to include covariates in the model that quantify the landscape structures that determine the types of organisms communicating in the soundscape (Pijanowski et al. 2011b; Farina and Gage 2017). One example of successful soundscape maps of biological sound and anthropogenic noise was shown in a study of south-central Alaska from numerous landscape and anthropogenic measures, such as distance to rivers, distance to wetlands, aspect, and snowmobile activity (Mullet et al. 2016). In the landscape we have mapped, the habitat ranges from small patches of forest, to agricultural fields, small towns and villages, and suburban development. This range of habitats would be expected to support different assemblages of acoustically communicating species resulting in different biological sound. Accounting for these differences in landscape through the appropriate covariates could also better inform the radius used to calculate the road covariate, as the attenuation and transmission of sound is highly dependent on the structure of the landscape (Royle 2018). In this study we did not have data on important landscape variables and so a 600 m boundary was used as an estimate for how far anthropogenic noise will travel through a forested landscape based on Forman (2000) and MacLaren et al. (2018).

The PSD and acoustic indices derived from it (NDSI) have previously been shown to correlate

positively with anthropogenic activity (Fairbrass et al. 2017) and change with landscape structure (Fuller et al. 2015). Our soundscape maps support these findings as the PSD of the 0.5–2 kHz range that represents anthropogenic noise is highest in areas of high road concentration. However, the use of the PSD to represent anthropogenic noise and biological sound as we did in this study is limited in application to long-term soundscape monitoring studies. Depending on the location and time of day, numerous organisms communicate within the 0.5–2 kHz region that is designated as anthropogenic noise. In our study, a manual analysis of the recordings revealed only one species commonly singing within the 0.5–2 kHz region, supporting the use of the PSD values as proxies of biological sound and anthropogenic noise in this setting. In addition, we only recorded on days with no rain and minimal wind, minimizing the presence of abiotic sounds in the soundscape recordings, which is often not possible over vast spatio-temporal regions. Analysis of long-term monitoring of soundscapes where such assumptions are not valid requires alternative methods to distinguish between biological sound, anthropogenic noise, and abiotic sound. Convolutional neural networks have recently been utilized in a deep learning system called CityNet to predict the presence or absence of biological sound and anthropogenic noise in urban soundscapes (Fairbrass et al. 2019). Recent work using the spectral properties of sound as is done in Music Information Retrieval also shows promise for distinguishing between the three soundscape components (Bellisario and Pijanowski 2019; Bellisario et al. 2019). Further developing these methods, in conjunction with current acoustic indices and landscape measurements, could provide reasonable estimations of the relative amounts of biological sound, anthropogenic noise, and abiotic sound in a soundscape to allow for long-term monitoring of soundscapes and landscape health.

Like many ecological studies, data collection was limited as a result of resource availability (i.e., number of acoustic recorders). In this study, each soundscape was recorded on a single day between May and June for a total of 90 min. While this data paucity could have potential implications on inference, exploratory data analysis revealed that the specific day of the recording and time from sunrise did not explain large

amounts of variability in the relationships between the road covariate, anthropogenic noise, and biological sound, suggesting we are accurately capturing the relationship between anthropogenic and biological components in these soundscapes. Thus, we believe the available data and analysis provide valid inference about the soundscape dynamics in our study system and allow us to adequately explore the study objectives. Further, our proposed modeling framework is broadly applicable to settings where monitoring networks have additional data.

The proposed models were used to assess the extent to which available traffic data explains variability in anthropogenic noise and to quantify the functional relationship between anthropogenic noise and biological sound. Roads represent the dominant source of anthropogenic noise across the landscape in our study area, and have a large and growing impact around the world (Barber et al. 2011; Buxton et al. 2017). Understanding and predicting the sound impacts of roads on biological communities is an important focus of ecoacoustics researchers in many locations (Forman and Deblinger 2000; Herrera-Montes and Aide 2011; Mullet et al. 2016). The hierarchical Bayesian framework allows us to obtain parameter estimates, fitted values, and predicted values at new locations all within the same modeling framework. This framework can incorporate a range of soundscape data to explore a variety of topics, such as the relationship between biological sounds and anthropogenic impacts like road sound or habitat fragmentation, the monitoring of species density and population estimates using acoustic recordings, and the recovery of environments to natural/anthropogenic disturbances. Ecologists, conservation biologists, urban planners, and road engineers all have an interest in these questions. Utilization of such a broadly applicable modeling framework will greatly improve our ability to make inference regarding the ways anthropogenic noise contributes to the soundscape and influences biological sound and the biodiversity that it represents.

Compliance with ethical standards

Conflict of interest All authors declare that they have no conflict of interest.

References

Banerjee S, Carlin B, Gelfand A (2014) Hierarchical modeling and analysis for spatial data. In: Cox DR, Hinkley DV, Rubin D, Silverman BW (eds) Monographs on statistics & applied probability, 2nd edn. Chapman & Hall/CRC, London

Barber JR, Burdett CL, Reed SE, Warner KA, Formichella C, Crooks KR, Theobald DM, Fristrup KM (2011) Anthropogenic noise exposure in protected natural areas: estimating the scale of ecological consequences. Landsc Ecol 26(1):1281–1295

Barber JR, Crooks KR, Fristrup KM (2010) The costs of chronic noise exposure for terrestrial organisms. Trends Ecol Evol 25(1):180–189

Bates D, Mächler M, Bolker B, Walker S (2015) Fitting linear mixed-effects models using lme4. J Stat Softw 67(1):1–48

Bellisario KM, Pijanowski BC (2019) Contributions of MIR to soundscape ecology. Part I: potential methodological synergies. Ecol Inform 51:96–102

Bellisario KM, VanSchaik J, Zhao Z, Gasc A, Omrani H, Pijanowski BC (2019) Contributions of MIR to soundscape ecology. Part II: spectral timbral analysis for discriminating soundscape components. Ecol Inform 51:1–14

Berliner ML (1996) Hierarchical Bayesian time series models. In: Skilling J (ed) Maximum entropy and Bayesian methods, vol 79. Springer, New York

Bobryk CW, Rega-Brodsky CC, Bardhan S, Farina A, He HS, Jose S (2016) A rapid soundscape analysis to quantify conservation benefits of temperate agroforestry systems using low-cost technology. Agrofor Syst 90(6):997–1008

Boelman NT, Asner GP, Hart PJ, Martin RE (2007) Multi-trophic invasion resistance in Hawaii: bioacoustics, field surveys, and airborne remote sensing. Ecol Appl 17(8):2137–2144

Brackenbury J (1978) Power capabilities of the avian sound producing system. J Exp Biol 78:163–166

Brooks SP, Gelman A (1998) General methods for monitoring convergence of iterative simulations. J Comput Graph Stat 7(4):434–455

Brumm H, Slabbekoorn H (2005) Acoustic communication in noise. Adv Study Behav 35(5):151–209

Buxton RT, Agnihotri S, Robin VV, Goel A, Balakrishnan R (2018a) Acoustic indices as rapid indicators of avian diversity in different land-use types in an Indian biodiversity hotspot. J Ecoacoust 2(1):1–17

Buxton RT, McKenna MF, Mennitt D, Fristrup K, Crooks K, Angeloni L, Wittemyer G (2017) Noise pollution is pervasive in U.S. protected areas. Science 356(1):531–533

Buxton RT, Meyer E, Clapp M, McKenna MF, Crooks K, Angeloni LM, Stabenau E, Wittemyer G (2018b) Efficacy of extracting indices from large-scale acoustic recordings to monitor biodiversity. Conserv Biol 32(5):1174–1184

Can A, Leclercq L, Lelong J, Defrance J (2008) Capturing urban traffic noise dynamics through relevant descriptors. Appl Acoust 69(12):1270–1280

Clark JS (2007) Models for ecological data. Princeton University Press, Princeton

Conesel BD, Muer TD, Yperman I, Botteldooren D (2005) The influence of traffic flow dynamics on urban soundscapes. Appl Acoust 66(2):175–194

Cressie N, Calder CA, Clark JS, Hoef JMV, Wikle CK (2009) Accounting for uncertainty in ecological analysis: the strengths and limitations of hierarchical statistical modeling. Ecol Appl 19(3):553–570

Fahrig L, Rytwinski T (2009) Effects of roads on animal abundance: an empirical review and synthesis. Ecol Soc 14(1):21

Fairbrass AJ, Firman M, Williams C, Brostow GJ, Titheridge H, Jones KE (2019) CityNet: deep learning tools for urban ecoacoustic assessment. Methods Ecol Evol 10(2):186–197

Fairbrass AJ, Rennert P, Williams C, Titheridge H, Jones KE (2017) Biases of acoustic indices measuring biodiversity in urban areas. Ecol Indic 83:169–177

Farina A (2018) Ecoacoustics: a quantitative approach to investigate the ecological role of environmental sounds. Mathematics 7(21):1–16

Farina A, Gage SH (2017) Ecoacoustics: the ecological role of sounds. Wiley, Hoboken

Ferrari SL, Cribari-Neto F (2004) Beta regression for modelling rates and proportions. J Appl Stat 31(7):799–815

Forman RTT (2000) Estimate of the area affected ecologically by the road system in the United States. Conserv Biol 14(1):31–35

Forman RTT, Deblinger RD (2000) The ecological road-effect zone of a Massachusetts (U.S.A) suburban highway. Conserv Biol 14:36–46

Forman RT, Sperling D, Bissonette JA, Clevenger AP, Cutshall CD, Dale VH, Fahrig L, France RL, Goldman CR, heanue K, Jones J, Swanson F, Turrentine T, Winter TC (2003) Road ecology: science and solutions. Island Press, Washington DC

Fuller S, Axel AC, Tucker D, Gage SH (2015) Connecting soundscape to landscape: which acoustic index best describes landscape configuration? Ecol Indic 58(1):207–215

Gelman A, Carlin J B, Stern H S, Rubin D B (2004) Bayesian data analysis, 2nd edn. Chapman and Hall/CRC, London

Gneiting T, Raftery AE (2007) Strictly proper scoring rules, prediction, and estimation. J Am Stat Assoc 102(477):359–378

Hanks EM, Schliep EM, Hooten MB, Hoeting JA (2015) Restricted spatial regression in practice: geostatistical models, confounding, and robustness under model misspecification. Environmetrics 26(4):243–254

Herrera-Montes MI, Aide TM (2011) Impacts of traffic noise on anuran and bird communities. Urban Ecosyst 14:415–427

Hobbs, NT, Hooten, MB (2015). Bayesian models: a statistical primer for ecologists. Princeton University Press, Princeton, New Jersey.

Joo W, Gage SH, Kasten EP (2011) Analysis and interpretation of variability in soundscapes along an urban-rural gradient. Landsc Urban Plan 103(3):259–276

Jordan A, Krueger F, Lerch S (2018) Evaluating Probabilistic Forecasts with scoringRules. J Stat Softw (forthcoming)

Kasten EP, Gage SH, Fox J, Joo W (2012) The remote environmental assessment laboratory's acoustic library: an archive for studying soundscape ecology. Ecol Inform 12(1):50–67

Katti M, Warren PS (2004) Tits, noise and urban bioacoustics. Trends Ecol Evol 19(3):109–110

Knudsen E, Konishi M (1979) Mechanisms of sound localization in the Barn Owl Tyto alba. J Comp Physiol 133(1):13–21

Ligges U, Krey S, Mersmann O, Schnackenberg S (2018) tuneR: Analysis of Music and Speech

Lunn D, Barrett J, Sweeting M, Thompson S (2013) Fully bayesian hierarchical modelling in two stages, with application to meta-analysis. J R Stat Soc 62(4):551–572

MacLaren AR, Crump PS, Royle JA, Forstner MRJ (2018) Observer-free experimental evaluation of habitat and distance effects on the detection of anuran and bird vocalizations. Ecol Evol 8(24):12991–13003

Marler P, Slabbekoorn H (2003) Nature's music. Elsevier, Amsterdam

McClure CJW, Ware HE, Carlisle J, Kaltenecker G, Barber JR (2013) An experimental investigation into the effects of traffic noise on distributions of birds: avoiding the phantom road. Proc R Soc Biol Sci 280:20132290

McGregor P (2005) Animal communication networks. Cambridge University Press, Cambridge

Merchant ND, Fristrup KM, Johnson MP, Tyack PL, Witt MJ, Blondel P, Parks SE (2015) Measuring acoustic habitats. Methods Ecol Evol 6(3):257–265

Mullet TC, Gage SH, Morton JM, Huettmann F (2016) Temporal and spatial variation of a winter soundscape in south-central Alaska. Landsc Ecol 31(5):1117–1137

Napoletano BM (2004) Measurement, quantification and interpretation of acoustic signals within an ecological context. Michigan State University, East Lansing

Neuweiler G (1989) Foraging ecology and audition in echolocating bats. Trends Ecol Evol 4(6):160–166

NYS Department of Transportation (2018) New York State Department of Transportation Traffic Data Viewer. https://www.dot.ny.gov/tdv. Accessed 10 April 2019

NYS ITS GIS Program Office (2019) New York State GIS Clearinghouse. https://gis.ny.gov. Accessed 10 April 2019

Oberweger K, Goller F (2001) The metabolic cost of birdsong production. J Exp Biol 204:3379–3388

Ortega CP (2012) Effects of noise pollution on birds: a brief review of our knowledge. Ornithol Monogr 74:6–22

Parris KM, Schneider A (2008) Impacts of traffic noise and traffic volume on birds of roadside habitats. Ecol Soc 14(1):29

Patricelli GL, Blickley JL (2006) Avian communication in urban noise: causes and consequences of vocal adjustment. Auk 123(3):639–649

Phillips JN, Derryberry EP (2018) Urban sparrows respond to a sexually selected trait with increased aggression in noise. Sci Rep 8(1):1–10

Pieretti N, Farina A, Morri D (2011) A new methodology to infer the singing activity of an avian community: the Acoustic Complexity Index (ACI). Ecol Indic 11(3):868–873

Pijanowski BC, Farina A, Gage SH, Dumyahn SL, Krause BL (2011a) What is soundscape ecology? An introduction and overview of an emerging science. Landsc Ecol 26(9):1213–1232

Pijanowski BC, Villanueva-Rivera LJ, Dumyahn SL, Farina A, Krause BL, Napoletano BM, Gage SH, Pieretti N (2011b) Soundscape ecology: the science of sound in the landscape. BioScience 61(3):203–216

Potvin DA (2017) Coping with a changing soundscape: avoidance, adjustments, and adaptations. Anim Cognit 20(1):9–18

Project Remote (2019) Remote Statistics. https://www.projectremote.com/. Accessed 25 Mar 2019

R Core Team (2019) R: a Language and Environment for Statistical Computing. R Foundation for Statistical Computing, Vienna, Austria

Rajan SC, Athira K, Jaishanker R, Sooraj NP, Sarojkumar V (2019) Rapid assessment of biodiversity using acoustic indices. Biodivers Conserv 28(8–9):2371–2383

Rice WR (1982) Acoustical location of prey by the Marsh Hawk: adaptation to concealed prey. Auk 99(3):403–413

Ridley AR, Child MF, Bell MB (2007) Interspecific audience effects on the alarm-calling behaviour of a kleptoparasitic bird. Biol Lett 3(6):589–591

Roberts GO, Rosenthal JS (2009) Examples of adaptive MCMC. J Comput Graph Stat 18(2):349–367

Royle JA (2018) Modeling sound attenuation in heterogeneous environments for improved bioacoustic sampling of wildlife populations. Ecol Indic 58(1):1–13

Slabbekoorn H, Ripmeester EAP (2008) Birdsong and anthropogenic noise: implications and applications for conservation. Mol Ecol 17(1):72–83

Sloan JL, Hare JF (2008) The more the scarier: adult Richardson's ground squirrels (Spermophilus richardsonii) assess response urgency via the number of alarm signallers. Ethology 114(1):436–443

Snow N P, Zhang Z, Finley A O, Rudolph B A, Porter W F, Williams D M, Winterstein S R (2018) Regional-based mitigation to reduce wildlife–vehicle collisions. J Wildl Manag 82(4):756–765

Sueur J, Aubin T, Simonis C (2008) Seewave: a free modular tool for sound analysis and synthesis. Bioacoustics 18:213–226

Templeton C N (2006) Antipredator defenses in birds and mammals. interspecific interactions. Q Rev Biol 81(3):309–310

Tennessen JB, Parks SE, Langkilde T (2014) Traffic noise causes physiological stress and impairs breeding migration behaviour in frogs. Conserv Physiol 2(1):1–8

Vehtari A, Gelman A, Gabry J (2017) Practical Bayesian model evaluation using leave-one-out cross-validation and WAIC. Stat Comput 27(5):1413–1432

Vehtari A, Lampinen J (2002) Bayesian model assessment and comparison using cross-validation predictive densities. Neural Comput 14(10):2439–2468

Villanueva-Rivera LJ, Pijanowski BC (2018) Soundecology: soundscape ecology. R Package Version 1(3):3

Villanueva-Rivera LJ, Pijanowski BC, Doucette J, Pekin B (2011) A primer of acoustic analysis for landscape ecologists. Landsc Ecol 26(9):1233–1246

Warren PS, Katti M, Ermann M, Brazel A (2006) Urban bioacoustics: it's not just noise. Anim Behav 71(3):491–502

Welch PD (1967) The use of fast fourier transform for the estimation of power spectra: a method based on time averaging over short, modified periodograms. IEE Trans Audio Electroacoust 15:70–73

Wildlife Acoustics (2012) Wildlife Acoustics. https://www.wildlifeacoustics.com/. Accessed 1 May 2019

Wood WE, Yezerinac SM (2006) Song sparrow song varies with urban noise. Auk 123(3):650–659